

EXPERIENCE IN RESEARCH, DEVELOPMENT, CONSTRUCTION AND COMMISSIONING OF NORMALLY CONDUCTING ACCELERATING STRUCTURES

L.V. Kravchuk, V.V. Paramonov *, INR of the RAS, Moscow, 117312, Russia

Abstract

The experience and results of research, development, construction and start of normally conducting accelerating structures for high intensity hadron linear accelerators at medium and high energies is summarized. Created methods and obtained results provided construction and start of operation of accelerating system in INR H- linac with designed energy 600 MeV. The research results allow generalize the properties of high energy structures and develop methods and criteria for improvements. Basing on research results, the high energy accelerating structure, which surpasses analogues in the total list of parameters, is proposed and tested.

INTRODUCTION

Instead of progress in development of superconducting structures for high energies, the normal conducting structures have the high value for high energy intense hadron linacs. The report presents briefly the main steps and INR results in this activity.

DAW CONSTRUCTION FOR INR LINAC

INR activity in accelerating structures originates from construction of accelerating system for high energy part of INR linac, Fig. 1. This system consists of 27 four-tanks cavities, operating at $f_a = 991$ MHz. DAW tanks contain from $N_m = 18$ to $N_m = 27$ DAW modules, see Fig. 3a. The total number of DAW modules in the system is ~ 2400 and the system length is $\approx 300m$.

DAW structure, invented by V.G. Andreev, [1], for INR



Figure 1: DAW accelerating structure in the INR linac.

linac was developed and tested in RTI AS USSR and the framework technology was established. The first three steps – hot sludge to $\approx 500mm$ blanks from 170mm OFC rods, pre-forming with stamping and draft pre-turn were performed in industry under INR and RTI monitoring. Another steps of construction, starting from accurate processing and continuing through RF tuning, brazing of DAW tanks and finishing with system commissioning, were performed by INR in-house. For mass production, all steps in construction, such as reasonable and motivated tolerances for DAW modules treatment, fast and precise RF tuning of DAW tanks, HOM displacement and so on, were optimized and improved. In the DAW construction there were no DAW modules lost due to non-compliance.

Individual RF tuning for frequencies of operating f_a and coupling f_c modes for DAW modules is not required, due to coupling coefficient $k_c \sim 40\%$ of the structure. DAW tanks were tuned in assembly of N_m modules. Coupling mode can not be excited in DAW tanks and to close the stop band non direct methods for stop band width $\delta f = f_c - f_a$ definition are required. Due to large k_c , DAW dispersion curve in the f_a vicinity is essentially not linear and linear approximation from nearest modes $\delta f = f_u^{(1)} + f_d^{(1)} - 2f_a$, tolerable for structures with $k_c \sim 5\%$, Side Coupled Structure (SCS) and Annular Coupled Structure (ACS), results in $\delta f \sim 1MHz$. High order approximations for δf definition were developed for DAW tanks tuning, [2], resulting in $\delta f \leq 100kHz$. Basing on DAW particularities, the optimized procedure for tanks tuning was developed, [3], minimizing number of tuning operations.

The High Order Modes (HOM) with field variations on

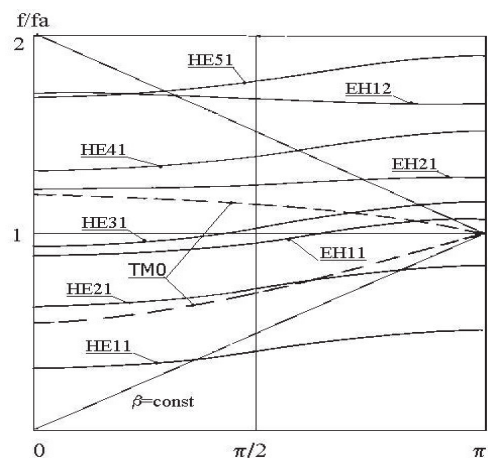


Figure 2: HOM dispersion diagram for the DAW, $\beta = 0.43$.

azimuth in f_a nearest vicinity for DAW were found in experiments and later classified in simulations [4], [5]. Calculated in 2D approximation dispersion diagram for DAW, $\beta = 0.43$ is shown in Fig. 2. All time in f_a vicinity exit EH_{11} and HE_{31} modes. Different methods for HOM displacement were considered [6], resulting in T-slots addition in disks, Fig. 3a. T-slots are selective resonant elements,

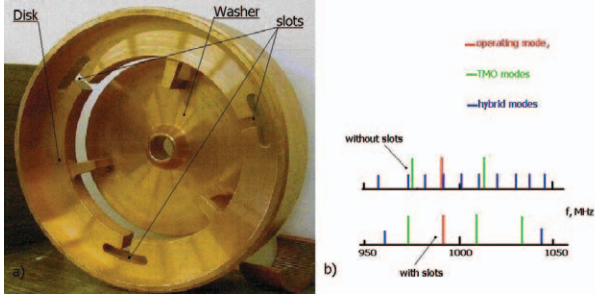


Figure 3: DAW module with T-slots (a) and modes spectrum in f_a vicinity without and with T-slots, (b).

which are tuned close to the operating frequency f_a , have no coupling with operating mode, weak coupling with another TM_0 modes, and a strong coupling with HOM. The result of T-slots interaction with HOMs in DAW is shown in Fig. 3b.

The beam break up in multi-sectional ion linac has very high current threshold, [7], and cumulative emittance growth due to beam interaction with HOMs for the designed current 50 mA is less than the same effect due to focusing elements misalignment, [8].

The distribution of electric field in large DAW and DTL cavities were performed by bead pull technique. To reduce random errors in measurements for large multi gap cavities, the size of spherical bead should be reasonably large. If bead diameter is comparable with accelerating gap length, the classical Slatter formula [9], derived for uniform infinite field, becomes a first approximation. The study of systematic error for bead pull measurements has been performed, [10], and bead diameters were chosen to limit systematic error to $\leq 0.2\%$ for measurements in DTL cavities and to $\leq 0.1\%$ in DAW cavities.

The total set of 110 DAW tanks was constructed and tuned to operating frequency with average, over set, value of standard deviation for E_z distribution $\approx 0.65\%$, [11]. All 27 DAW cavities four DAW tanks and three coupling bridges also were tuned for operating frequency and deviation of average E_z value between tanks $\leq 0.5\%$, [12]. Cavities were conditioned for operating level of RF power. The methods to pass fast the multipacktor discharge areas were developed in mass commissioning. The first beam acceleration was obtained in 1991.

METHODOLOGICAL DEVELOPMENTS

In the development and construction of accelerating structures the adequate software serves as cost reducing

tool of numerical experiments. Maintenance of DAW construction stimulated development, in collaboration with IHEP and JINR, the set of very fast and precise finite elements multi tasks software, [13], for simulations in 2D approximation. To maintain structure commissioning, the software for multipacting discharge study has been developed, [14]. For complete analysis of accelerating structures, operating with heavy RF power dissipation, the closed chain for simulations of RF parameters, dissipated RF power in the structure surface, flow and heat exchange simulation in cooling channels, thermal stress and deformations in the structure body and resulting changes in RF parameters, was developed [15] basing on ANSYS software. Very powerful tools for structures development are managing add-ins over software for data libraries storage, [16].

For generalization of physical processes description in

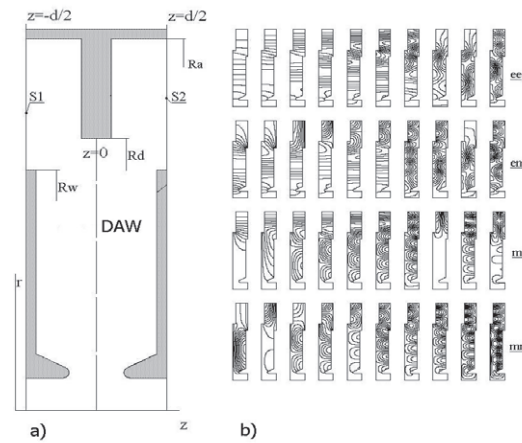


Figure 4: The geometry of one DAW period (a) and electric field distributions for 0 and π modes, simulated in different combinations of boundary conditions **ee**, **mm**, **em**, **me** (b).

different structures, the method of field description in periodical structures was developed, [17] and realized in an additional code. Let us consider just one period of the structure, for example, DAW in Fig. 4a. Using powerful modern software, let us simulate and store for sets of field distributions and frequencies in different combinations of boundary conditions (electric **e** and magnetic **m**) for 0 and π modes **ee**, **mm** and **em**, **me**, respectively, Fig. 4b. In structures with mirror symmetry just one half of the period is sufficient for such simulations. Considering the travelling wave with the phase advance θ at the period d , let us expand the real and the imaginary components of travelling field in the sets over stored basis of 0 and π modes with unknown coefficients c_n in such expansion, $\Re \vec{E} = \sum_n^{Nee} c_n^{ee} \vec{E}_n^{ee} + \sum_n^{Nem} c_n^{em} \vec{E}_n^{em}$, $\Im m \vec{E} = \sum_n^{Nme} c_n^{me} \vec{E}_n^{me} + \sum_n^{Nmm} c_n^{mm} \vec{E}_n^{mm}$. Applying Floquet boundary conditions at the period ends, $z = 0, z = d$ and using variational approach we obtain the symmetrical

eigenvalue problem

$$A(\theta)C - k^2 BC = 0, \quad (1)$$

where $A(\theta)$, B are square matrices with elements representing interaction of fields of basis elements, [17]. Specifying θ and solving problem (1) we define both frequency and field distribution for any $0 \leq \theta \leq \pi$. The equation (1) is the dispersion equation of the structure under consideration. The detail view of matrices $A(\theta)$ and B in (1) depends on the symmetry of the considered structure. All high energy structures, schematically shown in Fig. 5 have operating π mode and mirror symmetry plane in the middle of accelerating gap. Instead of quite different geometry and technical solutions, all these structures have the common dispersion equation (1), [18]. Even restricted with four modes, this

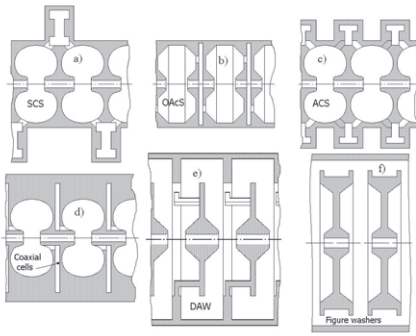


Figure 5: High energy compensated accelerating structures

equation describes well operating dispersion curve for all compensated high energy structures, including non symmetrical DAW curve. Considering just nearest vicinity of operating point f_a and restricting just with two interacting modes accelerating \vec{E}_a and coupling \vec{E}_c , we obtain the local dispersion equation,

$$(f_a^2 - f^2)(f_c^2 - f^2) - \left(\frac{f_a f_c k_c \sin \xi}{2}\right)^2 = 0, \quad \xi = \pi - \theta \quad (2)$$

which is valid for all compensated structures, and derive the expression for group velocity β_g (or coupling coefficient k_c).

$$\beta_g = \left| \frac{\pi \beta \int_{V_1} (\epsilon_0 \vec{E}_a \vec{E}_c - \mu_0 \vec{H}_a \vec{H}_c) dV}{4W_0} \right| = \frac{\beta \pi k_c}{4}, \quad (3)$$

The behaviour for mode frequencies and field distributions in the vicinity of operating mode were investigated in details illustrating both particularities of structures and common relationships too, [19]. The changes in field distributions and another parameters of these modes during structure tuning becomes clearly seen. Basing on the developed approach the coupling mode excitation due to beam loading [20], transient and tuning errors were studied, resulting in some deviations, which are more sensible physically, from the results, obtained by coupled circuits model [21]. Possibility of multipactoring discharge in coupling cells for

ISBN 978-3-95450-170-0

slot coupled SCS, ACS and OACS due to coupling mode excitation was studied [22] and methods for k_c increasing with the minimal Z_e drop by slot shape optimization were formulated [23]. For structures operating with heavy RF power dissipation criteria for thermo-mechanical stability were summarized, [24].

These developments are valid for a wide family of accelerating structures and provide complete set of approaches, recommendations and limitations in the research, development and improvement of accelerating structures. Joint with understanding of practical problems, it provides the reliable base for another developments.

COLLABORATING ACTIVITY

The results and experience of INR activity in investigation, construction and commissioning was implemented during construction and commissioning of warm part of the SNS linac, [25]. The total set of obtained results, developed methods and approaches was used in the development of physical design of ACS structure for J-PARC linac. Invented in USSR, ACS was strongly improved in KEK during JHP program under leadership of Y. Yamazaki for operating frequency $f_a = 1296 MHz$.

For J-PARC operating frequency $f_a = 972.0 MHz$ pre-



Figure 6: ACS half cells for J-PARC linac

vious JHP ACS has been deeply reconsidered. The total set of developed methods and approaches has been applied for cells optimization and mutual fitting, coupling slots arrangement and cooling study in order do not lose, only improve, achieved performances and to provide RF efficient, compact, balanced cost effective design ensuring reliable stable operation in linac, [26, 27]. The optimized ACS cells for J-PARC linac are shown in Fig. 6. Later some improvements were introduced in cells design for cost reduction in mass production, [28] and total 21 ACS cavities, consisting each of two ACS tanks and one bridge cavity, were constructed. With the robust design and high quality of manufacturing, all ACS cavities were conditioned for operating parameters relatively fast, [29], and stable operate now in J-PARC linac.

CDS DEVELOPMENT

The Cut Disk Structure (CDS) initially was proposed for electron linac, $\beta = 1$, [24],[30]. Topologically CDS looks,

Fig. 7, very similar to well known slot coupled OAcS, see Fig. 5, but realizes quite another concept. The shape of accelerating CDS cells is optimized for the maximal Z_e value, and coupling cell is formed so, that magnetic field H_c has no own space in coupling cell and is extruded into accelerating cell, with necessity resulting in large β_g value, according (3), without associated, for coupled slot structures, Z_e drop.

CDS concept was proven in the cold model measurements,

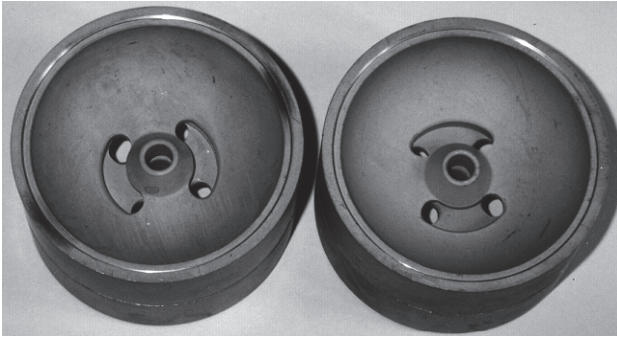


Figure 7: CDS cells for cold model test.

showing calculated $k_c = 0.22$ and Z_e/Q values, [31]. For further developments we adopt four windows CDS option with windows opening $\sim 45^\circ$ in order to improve vacuum conductivity, increase Z_e value, further reduce possibility of multipactor discharge in coupling cells. Basing on CDS, the booster cavity to increase electrons energy in the Photo Injector Test Facility (PITZ), DESY, Zheuthen, was developed in INR, [31] to operate with $\beta = 1$, $f_a = 1300\text{MHz}$, designed accelerating gradient up to 14MeV/m and dissipation heat load up to 17kW/m , Fig. 7. In cavity development and construction all set of our methods and approaches was used. For higher structure reliability for four windows CDS option the cooling circuit design without brazed water-vacuum joints was developed. The booster cavity, Fig. 8, was constructed in DESY, tuned, conditioned [32] and now is in operation at the PITZ beam line, [33].

With operating PITZ booster cavity CDS operational reli-

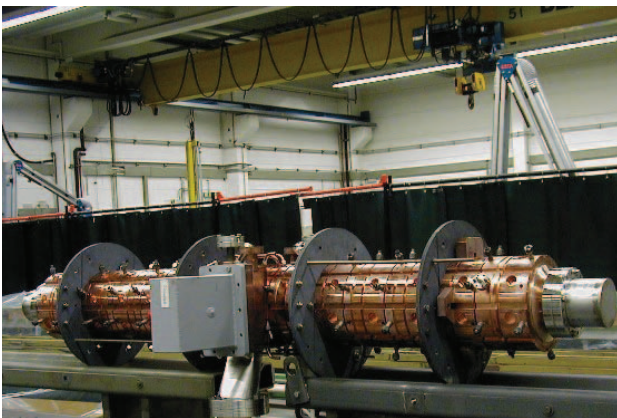


Figure 8: CDS booster cavity for PITZ

ability is proven.

Due to design idea, transverse CDS dimensions are defined by accelerating cell radius $R_c \sim 0.37\lambda$. Comparison of different structures in transverse dimensions is shown in Fig. 8a for the same operating frequency f_a and same β . Due to small R_c , CDS has no HOM problem. The nearest HOM modes are placed at frequencies $\sim 1.5f_a$. Also with smaller dimensions, CDS is cheaper in the construction, starting from smaller amount of row OFC material and continuing with relaxed requirements to treatment with modern NC machines. Expected CDS parameters were es-

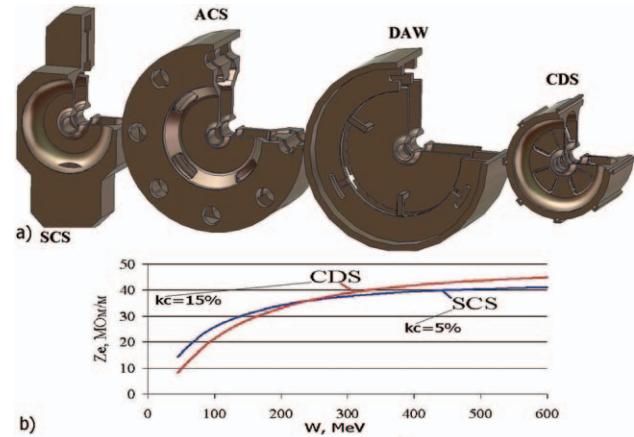


Figure 9: Structures comparison in dimensions (a) and efficiency (b).

timated and for lower β value, assuming proton acceleration from energy $\sim 100\text{MeV}$, [35]. Assuming the application in the intense proton linac with the heat loading $\sim 15\text{kW/m}$, resulting in the necessity of cooling channels in the walls between accelerating and coupling cells and the total thick web, the calculated Z_e values are shown in Fig. 8b. In for windows CDS option with slots opening $\sim 45^\circ$ the quite sufficient value $k_c \sim 0.15$ obeys naturally. The big CDS coupling windows, Fig. 8a replace the part of the accelerating cell surface with the high RF loss density. It explains higher Z_e value for high energies. For lower $\beta \leq 0.55$ for the present CDS design the original disadvantage the thick web determine Z_e reduction, as compared to another structures in Fig. 8a. Results of simulations show, if accelerating structure is applied for for proton acceleration from 100MeV to $\geq 400\text{MeV}$ the present CDS in total overlaps another structures in RF efficiency. Also, as recent estimations show, that with more complicated cell shape, but realistic for modern NC tools, we can improve CDS efficiency for low β , eliminating this disadvantage. The small transverse dimensions allow CDS application for relatively low operating frequency $f_a = 352\text{MHz}$, [36]. For such applications CDS efficiency and field stability can be decisive arguments. The summarized comparison of CDS parameters in values and in relative ranking, with another structures, is given in the Table 1.

As one can see, in the total set of parameters, both physical

Table 1: Thermo-mechanical effects

Structure	SCS	ACS	DAW	CDS
$Z_e/Z_{eSCS}, \%$	100	~ 99	~ 95	85 – 107
$k_e, \%$	~ 5	~ 5	~ 45	~ 15
$P_h, kW/m$	~ 10	≤ 60	≤ 6	≤ 35
R_c/λ	0.7	0.7	0.7	0.37
Vacuum cond.	2 – 4	2 – 4	1	2 – 4
HOM, rank	2	3	4	1
RF tuning				
before braz.	indiv.	indiv.	total	total
after braz.	a/c	no/c	no/no	a/no
water-vac.	yes	yes	yes	no

and technological, CDS represents the balanced optimized option. This structure is promising candidate for applications in attractive normal conducting linacs.

SUMMARY

In the INR research activity in normal conducting accelerating structures the complete set of methods, approaches for investigation, development and construction of accelerating structures was developed. Results of this activity are realized in the constructed, tuned, commissioned and operating accelerating system of the INR hadron linac, are implemented in the design, construction and commissioning of similar linacs in foreign laboratories. Guiding this basements results, attractive proposal for different future application is generated, investigated and tested.

ACKNOWLEDGMENT

The authors warmly tank a lot of our colleagues in INR, MRTI, DESY, KEK, J-PARC, SNS for good collaborations in accelerating structures development and construction.

REFERENCES

- [1] V.G. Andreev, Journal of Technical Physics, v. 41, n. 4, p. 788-795, 1971, (in Russian)
- [2] L. Kravchuk, V. Paramonov et.al., IEEE Trans. on Nucl. Sci., NS-32, n.5, p. 2818-2820, 1985
- [3] L. Kravchuk, G. Romanov, Preprint INR AS USSR, P-0334, Moscow, 1984 (in Russian).
- [4] V. Paramonov, Journal of Technical Physics, v. 43, n. 5, p. 956, 1983, (in Russian)
- [5] V. Andreev, L. Kravchuk, V. Paramonov et.al., NIM, A, v. 204, p. 285, 1983
- [6] V. Andreev, L. Kravchuk, V. Paramonov et.al., IEEE Trans. on Nucl. Sci., NS-32, n.5, p. 3575, PAC 1985, 1985
- [7] P. Ostroumov, L. Kravchuk, V. Paramonov et.al., Proc. Linac 1984, p. 392, 1984
- [8] P. Ostroumov, L. Kravchuk, V. Paramonov et.al., IEEE Trans. on Nucl. Sci., NS-32, n.5, p. 2368, PAC 1985, 1985

- [9] L. Maier, J. Slatter, Journal of Applied Physics, v. 23, n.1, p.68, 1952
- [10] L. Kravchuk, P. Ostroumov, V. Paramonov et.al., Proc. Linac 1990, p. 120, 1990
- [11] S. Esin, L. Kravchuk, V. Paramonov et.al., Proc. Linac 1988, p. 657, 1988
- [12] S. Esin, L. Kravchuk, G. Romanov et.al., Proc. EPAC 1990, p. 506, 1990
- [13] I. Gonin, V. Gorbunov, V. Paramonov, Proc. EPAC 1990, p. 1249, 1990
- [14] L. Kravchuk, G. Romanov, S. Tarasov, Proc. Linac 1993, p. 465, 1992
- [15] S. Joshi, V. Paramonov, A. Skasyrskaya, Proc. Linac 2002, p. 216, 2002
- [16] V. Paramonov, Proc. Linac 1996, p. 493, 1996
- [17] V. Paramonov, I. Gonin, Proc. Linac 2000, p. 804, 2000
- [18] V. Paramonov, Proc. Linac 2002, p. 410, 2002
- [19] V. Paramonov, Proc. Linac 2000, p. 401, 2000
- [20] V. Andreev, V. Paramonov, IEEE Trans. on Nucl. Sci., NS-32, n.3, p. 1702, PAC 1985, 1985
- [21] E.A. Knapp et.al., Rev. Sci. Instr., v. 38, n.11, p. 22, 1967
- [22] V. Paramonov, S. Tarasov, Proc. Linac 1998, p. 971, 1998
- [23] V. Paramonov, Proc. Linac 2008, p. 61, 2008
- [24] V. Paramonov, Proc. of the 15-th RuPAC, Protvino, IHEP, v. 1, p. 156, 1996 (in Russian).
- [25] S. Handerson, L. Kravchuk et.al., NIM,A, v. 763, p. 610-673, 2014
- [26] V. Paramonov, KEK Report 2001-14A, KEK, 2001
- [27] H. Ao, V. Paramonov, Y. Yamazaki et.al., Proc. Linac 2002, p. 234, 2002
- [28] H. Ao, Y. Yamazaki, V. Paramonov et.al., Proc. Linac 2008, p. 915, 2008
- [29] H. Ao et.al., Proc. Linac 2014, THPP089, 2014
- [30] V. Paramonov. Proc. PAC1997, v.3, p.2959, 1997.
- [31] V. Paramonov, L.V. Kravchuk, V.A. Puntus. Proc. Linac1998, p. 579, 1998.
- [32] V. Paramonov, N. Brusova, Proc. Linac2004, p. 204, 2004.
- [33] A. Naboka, V. Paramonov, F. Stephan et.al., Proc. Linac2010, p. 241, 2011
- [34] M. Krasilnikov, F. Stephan, V. Paramonov et.al., Phys. Rev. ST Accel. Beams v. 15, n. 10, 100701, 2012
- [35] V. Paramonov, Proc 22 RuPac2010 p. 65, 2010
- [36] V. Paramonov, Proc. Linac2014, MOPP125, 2014